Coarse-grained simulation of transmembrane peptides in the gel phase

Ibrahim H. Al-Lehyani[a,b], John M. A. Grime[c,d], Matthew Bano[e], Kim McKelvey[e], Michael P. Allen[f,*]

[a] *Department of Physics, King Abdulaziz University, Jeddah, Saudi Arabia*
[b] *The National Center for Mathematics and Physics, King Abdulaziz City for Science and Technology, Riyadh, Saudi Arabia*
[c] *Department of Chemistry, University of Chicago, 5735 S Ellis Ave, Chicago, IL 60637, USA*
[d] *Mathematics and Computer Science Division, Argonne National Laboratory, 9700 South Cass Avenue, Building 240, Argonne, IL 60439-4844, USA*
[e] *MOAC Doctoral Training Centre, University of Warwick, Coventry, CV4 7AL, United Kingdom*
[f] *Department of Physics, University of Warwick, Coventry, CV4 7AL, United Kingdom*

Abstract

We use Dissipative Particle Dynamics simulations, combined with parallel tempering and umbrella sampling, to investigate the potential of mean force between model transmembrane peptides in the various phases of a lipid bilayer, including the low-temperature gel phase. The observed oscillations in the effective interaction between peptides are consistent with the different structures of the surrounding lipid phases.

Keywords:

Dissipative-particle-dynamics,molecular-dynamics,bilayer,peptide

*Corresponding Author

Email addresses: iallehyani@kau.edu.sa (Ibrahim H. Al-Lehyani), jgrime@uchicago.edu (John M. A. Grime), m.p.allen@warwick.ac.uk (Michael P. Allen)

1. Introduction

A cell membrane is a complex structure whose dynamic and structural properties extend over many length- and time-scales. A key element of the membrane is a flexible bilayer: a self-assembled structure consisting of a large number of types of lipid, of which the phospholipids are the most abundant type. Proteins comprise the second most commonly found component in the membrane, embedded in the lipid bilayer, or attached to its surface, thus affecting the morphology and properties. Our interest in this paper lies in integral membrane proteins containing a well-defined hydrophobic transmembrane section, which spans the double layer. One of the functions of such proteins is to form a passage for charged and polar molecules across cell membranes. Frequently, a pore is formed by aggregation of a small number of protein monomers, and so the interactions between proteins are of great interest [1, 2]. Different proteins interact differently with each other and with lipids. Their mutual interactions can be direct or mediated through the lipids in the membrane [3], and this latter effect is the subject of this paper.

The membrane is stabilized through the usual atomic and molecular interactions (electrostatic, van der Waals, and hydrogen bond interactions), but the main force affecting the structure and the dynamics of proteins within membranes is the hydrophobic mismatch [4]. Transmembrane proteins typically consist of a hydrophobic part (for example, an α-helix or β-barrel) capped at both ends by hydrophilic head groups. When a protein is embedded in a lipid bilayer, the bilayer hydrophobic thickness and the hydrophobic length of the protein may or may not match; this affects the structure of the membrane locally around the protein in terms of the thickness of the

bilayer. The energy cost of exposing the hydrophobic part of the protein is so high that the hydrophobic effect can force a protein to tilt, bend, or even change its structure to avoid water. A range of experimental and theoretical techniques are in current use to improve our understanding of these effects [5].

The lipid bilayer can be in one of many phases, according to its temperature, pressure, and the types of lipid of which it consists. Naturally, in living cells, under ambient conditions, they are in a fluid, or liquid crystalline (L_α) phase where their tails are disordered and the molecules are highly mobile. At lower temperatures, a ripple phase ($P_{\beta'}$) may be observed, depending on the type of lipids present in the bilayer. The ripple phase has long-wavelength undulations of the bilayer and swelling in the membrane. The lipid tails are somewhat more ordered than in the L_α phase, and tilted with respect to the bilayer normal. At even lower temperatures, a tilted gel phase ($L_{\beta'}$) is observed, or, for lipids with smaller head groups, an untilted gel phase (L_β). In the gel, the lipid tails still show some residual disorder, and the dynamics is very sluggish. Finally, at still lower temperatures, a sub-gel phase (L_c) may be observed. This phase is characterized by tilted lipid tails with respect to the bilayer normal; the tails are highly ordered, adopting an all-trans zig-zag chain structure characteristic of crystalline alkanes.

In most cases, membrane proteins span the membrane as hydrophobic α-helices. Experimentally, it is very convenient to study the transmembrane section in isolation. WALP23 is a synthetic membrane peptide (a small model protein) that takes an α-helical conformation. It belongs to a family of proteins possessing a core of alternating hydrophobic leucine and alanine

residues, with hydrophilic tryptophan ends. Using atomic force microscopy (AFM), de Kruijff observed the surface organization and hexagonal packing of WALP23 peptides in the gel phase of a dipalmitoylphosphatidylcholine (DPPC) lipid bilayer [6]. Atomic force microscopy shows that the presence of the peptides in a supported bilayer of DPPC affects the morphology of the membrane. This article is part of an effort to understand and simulate a model of the packing of WALP23 peptides and their interactions in all phases of DPPC lipid bilayers. Our strategy is to calculate the potential of mean force (PMF) as a function of the temperature and the separation distance between the two peptides, by computer simulation. The PMF is an important concept and tool in the study of liquids and complex molecular systems [7]. Here, it measures the propensity of the peptides to attract or repel each other, including all the averaged effects of the surrounding and interposed lipids.

Simulation has been a major theoretical tool for studying the structure and the dynamics of biomembranes for at least thirty years [8]. Several recent reviews [9–11] give an excellent introduction to the field. Atomistic simulations are, in principle, capable of calculating all the properties and effects in membranes at all length- and time-scales [12] . When combined with experiment, they have shed some light on the various features affecting membrane-mediated protein interactions [13]. However, in practice, for membranes in water, with tens of thousands of degrees of freedom, these simulations are very slow. Such detailed molecular modelling can be restricted in sampling (due to limits of computer power) even when combined with special techniques [14, 15]. This problem becomes especially acute in

the lower-temperature phases, where the molecular mobility is very low, and it is difficult to effectively sample an equilibrium ensemble in a reasonable time. Many of these degrees of freedom might not be relevant, and integrating them out results in a substantial saving of simulation time. The resulting, coarse-grained, model can advance much faster in time, allowing the study of much slower, or larger-scale, processes [16]. Simulations of lipid membranes using extremely coarse-grained models, in which each particle represents many atoms, are much more efficient [10, 17, 18] and have given considerable insight into the interaction between embedded proteins [19–23].

We follow this highly-coarse-grained approach in this paper, and in particular we demonstrate that it is possible to obtain information about the membrane-mediated interactions between peptides, even in the highly challenging gel phase. In section 2 we describe the model and the simulation methods that we employ. We present our results in section 4, and conclusions in section 5.

2. Simulation Model

In this work, we use a mesoscale model pioneered, in the context of lipid simulations, by Smit and co-workers [10], based on the interaction potentials used in dissipative particle dynamics (DPD) simulations [24]. Each particle or bead represents a group of atoms or molecules (typically one bead for three or four molecules in the case of water). To mimic the effects of the degrees of freedom that are sacrificed during the coarse-graining process, a dissipative force $\mathbf{f}^{\mathrm{D}}$ and a random force $\mathbf{f}^{\mathrm{R}}$ are introduced into the equations of motion of the system, besides the conservative forces already present between beads.

The total force $\mathbf{f}_i$ on any bead i at any time is the collective sum of these forces,

$$\mathbf{f}_i = \mathbf{f}_i^{\mathrm{S}} + \mathbf{f}_i^{\mathrm{B}} + \sum_j \mathbf{f}_{ij}^{\mathrm{C}} + \mathbf{f}_{ij}^{\mathrm{D}} + \mathbf{f}_{ij}^{\mathrm{R}} \,. \tag{1}$$

The first two terms are intramolecular interactions, respectively due to bond-stretching and bond-bending potentials. The remaining sum, the non-bonded interactions, is taken over all neighbouring beads $j \neq i$ whose distance $r_{ij} = \big|\mathbf{r}_{ij}\big| = \big|\mathbf{r}_i - \mathbf{r}_j\big|$ from i lies within a cutoff distance $r_{ij} \leq r_{\mathrm{cut}}$. As is conventional, we shall use this distance as a unit of length $r_{\mathrm{cut}} = 1$ in everything that follows.

The interactions between beads within a molecule, due to bond-stretching Φ^{S} and bond-bending Φ^{B} potentials, take the forms

$$\Phi^{\mathrm{S}} = \sum_{\langle ij \rangle} \tfrac{1}{2}\kappa_{\mathrm{S}}\big(r_{ij} - r_{\mathrm{S}}\big)^2 \,, \quad \Phi^{\mathrm{B}} = \sum_{\langle ijk \rangle} \tfrac{1}{2}\kappa_{\mathrm{B}}\big(\theta_{ijk} - \theta_{\mathrm{B}}\big)^2 \,. \tag{2}$$

Here, the sums are over bonded pairs $\langle ij \rangle$ and triplets $\langle ijk \rangle$ in the molecular structure, r_{ij} is defined above, and the angle θ_{ijk} is defined by $\cos\theta_{ijk} = \hat{\mathbf{r}}_{ij} \cdot \hat{\mathbf{r}}_{jk}$, where the hat denotes a unit vector $\hat{\mathbf{r}} = \mathbf{r}/r$. Each of these potentials is specified by two parameters: a characteristic spring constant (κ_{S}, κ_{B}), and an equilibrium value (r_{S}, θ_{B}) at which the potential has its minimum. The corresponding forces are derived as usual: $\mathbf{f}_i^{\mathrm{S}} = -\nabla_i \Phi^{\mathrm{S}}$, $\mathbf{f}_i^{\mathrm{B}} = -\nabla_i \Phi^{\mathrm{B}}$, where ∇_i represents the gradient with respect to the coordinates $\mathbf{r}_i$.

The nonbonded part of the conservative force models the hydrophobic and hydrophilic interactions, and is given by the completely repulsive form

$$\Phi^{\mathrm{C}} = \sum_i \sum_{j>i} \tfrac{1}{2} a_{ij} w(r_{ij})^2 \,, \quad \text{where} \quad w(r) = \begin{cases} 1 - r & r < 1 \\ 0 & r > 1 \end{cases} \tag{3}$$

which leads to pairwise forces

$$\mathbf{f}_i^{\mathrm{C}} = \sum_{j \neq i} \mathbf{f}_{ij}^{\mathrm{C}} = \sum_{j \neq i} a_{ij} w(r_{ij}) \hat{\mathbf{r}}_{ij} \, . \tag{4}$$

Here a_{ij} is the maximum repulsion strength, and the weight function $w(r)$ is defined to vanish at the cutoff distance $r_{\mathrm{cut}} = 1$. In our models, all the cutoff distances are chosen to be equal, i.e. all the beads are effectively the same size. Different species are differentiated by the values of a_{ij}.

Together, the terms $\Phi = \Phi^{\mathrm{S}} + \Phi^{\mathrm{B}} + \Phi^{\mathrm{C}}$ constitute the potential energy part of the hamiltonian, which defines the equilibrium configurational distribution function in the canonical ensemble at temperature T, namely the Boltzmann distribution $\exp(-\Phi/k_{\mathrm{B}}T)$. The remaining dissipative ($\mathbf{f}_{ij}^{\mathrm{D}}$) and random ($\mathbf{f}_{ij}^{\mathrm{R}}$) forces preserve this distribution, and are fully described elsewhere [24, 25].

We adopt here the model of Venturoli and co-workers [26] which is a realization of DPD for the cell membrane to analyze a bilayer of DPPC lipids with embedded WALP23 peptides, in water. Five types of DPD beads are used: water w, lipid head h, lipid tail t, peptide end p, and peptide internal bead q. A water bead represents approximately three water molecules; we adhere to the convention that water beads interact with a repulsion $a_{\mathrm{ww}} = 25$, which defines the overall energy scale, such that a temperature $k_{\mathrm{B}}T = 1$ corresponds to ambient conditions [24]. (In the following, Boltzmann's constant k_{B} is set equal to unity). The repulsion parameters between the different bead types are listed in Table 1, and they are mainly taken from Ref. [26]. The exception is the repulsion between the protein hydrophobic groups and water, which we choose to set equal to the repulsion between the lipid tail groups and water.

	w	h	t	p	q
w	25	15	80	15	80
h	15	35	80	35	80
t	80	80	25	80	25
p	15	35	80	35	80
q	80	80	25	80	25

Table 1: Repulsion parameters a_{ij} between different types of DPD bead in the model

The DPPC lipid is represented by three hydrophilic head beads (h) and two tails each consisting of six hydrophobic beads (t), the $h_3(t_6)_2$ model of Kranenburg and Smit [17]. The lipid beads are connected by bonds of spring constant $\kappa_S = 100$ and an equilibrium distance of $r_S = 0.7$. Beside these bond-stretching terms, the lipid tails possess bending elasticity that is modelled by a spring constant of $\kappa_B = 6$ and an equilibrium angle of $\theta_B = 0°$ for successive bonds along each tail. In addition there is a bending potential with $\kappa_B = 6$ and $\theta_B = 90°$ at each head-tail junction.

WALP23 is an α-helical synthetic peptide with a radius of 2.3 Å, each turn of which contains 3.6 side groups, and contributes 5.4 Å to the length. Its total length is 34.5 Å, of which the hydrophobic part is 31.5 Å [27]. Based on the dimensions of an α-helix, the dimensions of the WALP23 peptide, and the structure of the α-helical protein used in DPD simulations by Venturoli, we model the WALP23 with 14 layers of DPD particles. There are four DPD particles, arranged in a square, per layer. The three layers at each end of the protein are hydrophilic particles (p), to properly anchor the WALP23 peptide across the lipid bilayer, and the other eight layers are hydrophobic

particles (q). Bonds between the beads in adjacent layers, and within each layer, of equilibrium bond length $r_{\mathrm{S}} = 0.7$, and spring constant $\kappa_{\mathrm{S}} = 400$, are used to keep the molecule together.

3. Methods

To study the behavior of the membrane over a range of temperatures, we use the technique known as parallel tempering or replica exchange sampling [28]. In this method, several DPD runs at a range of temperatures are performed in parallel. At regular intervals, a set of Monte Carlo moves is proposed that would allow systems with potential energies Φ and Φ', at adjacent temperatures T and T', to exchange their configurations. The moves are independently accepted with Metropolis-like acceptance probability

$$\min\bigl(1, \exp\{\Delta\beta\Delta\Phi\}\bigr)$$

where $\Delta\beta = (k_{\mathrm{B}}T')^{-1} - (k_{\mathrm{B}}T)^{-1}$ and $\Delta\Phi = \Phi' - \Phi$. On acceptance of such a move, the particle momenta are scaled in accordance with the corresponding temperatures [29]. The spacing of the temperatures is empirically adjusted to ensure reasonable acceptance rates (at least a few percent) between every adjacent pair. Typically, we use 64 replicas covering a temperature range $T = 0.2$ – 0.6. The simulations are run in parallel, with one processor per replica, using the message-passing interface (MPI) for all communications.

The simulations are conducted in cuboidal periodic boundary conditions, with the bilayer spanning the xy-plane. To ensure that the membrane is maintained in a state of zero tension, we also regularly apply Monte Carlo moves which change the cross-sectional area of the simulation box, while keeping the volume fixed [10].

To calculate the potential of mean force (PMF) of a pair of peptides within the membrane, the above techniques are combined with umbrella sampling of the peptide separation. A biasing potential is applied linking the centres of the peptides, $\mathbf{r}_A$ and $\mathbf{r}_B$:

$$\Phi^{\mathrm{U}} = \tfrac{1}{2}\kappa_{\mathrm{U}}\big(r_{AB} - r_{\mathrm{U}}\big)^2 \,,$$

with $r_{AB} = \big|\mathbf{r}_A - \mathbf{r}_B\big|$. This restricts the statistical distribution of the separation r_{AB} to a range (dictated by the spring constant κ_{U}) around the chosen value r_{U}, resulting in efficient sampling in that region. Many values of r_{U} are investigated independently in the desired range of separations. We found that a value of $\kappa_{\mathrm{U}} = 50$ and a spacing between successive values of $\Delta r_{\mathrm{U}} = 0.1$ gave a satisfactory overlap of the distributions. To be clear: for each value of r_{U} a complete set of parallel tempering simulations was carried out, to give well-sampled simulation results at each temperature, under the influence of the biasing potential. All the results for each temperature were then combined: the biasing distribution was removed, and the PMF (along with other properties) determined, using the weighted histogram analysis method (WHAM) [19, 30]. This calculates the optimum distribution over the whole range by calculating a weight for each individual biased simulation, so as to minimize the overall statistical errors in the combination process.

Several bilayer properties are measured in the simulation. The bilayer hydrophobic thickness d_{L} is defined as the distance, normal to the bilayer, between the average positions of lipid head groups in the two monolayers. For this purpose, we use the third head bead (closest to the tails) to represent the head group. The area per lipid A_{L} is the total cross-sectional area of the simulation box divided by half the number of lipids. The lipid tail order can

be defined in terms of the angle between the lipid tail and the bilayer normal θ as

$$S_{\text{tail}} = \tfrac{1}{2}\big\langle 3\cos^2\theta - 1\big\rangle. \tag{5}$$

A value of 1 corresponds to perfect alignment with the normal, 0 to random orientation in three dimensions, and -0.5 to random orientation in the plane of the bilayer. The tilt angle χ_{tilt} of the WALP23 peptide is defined by averaging the cosine of the angle χ between the peptide axis and the bilayer normal

$$\cos\chi_{\text{tilt}} = \Big\langle \big|\cos\chi\big| \Big\rangle. \tag{6}$$

The effect of the peptide on the bilayer can be measured as a change of lipid bilayer thickness as a function of distance in the plane. This is accumulated in the simulation as a histogram, in a series of concentric circles centered on the peptide position; since the peptide can be tilted, the two lipid monolayers are treated separately in this analysis.

4. Results and Discussion

As a preliminary check, the DPPC lipid bilayer was simulated with 219 lipid molecules and 6657 water beads. The initial simulation box size was $12\times12\times24$. Starting with the lipids and water particles randomly positioned, a simulation was run on a single processor at $T = 0.6$, without parallel tempering or the zero surface tension method, until a lipid bilayer formed which was then used as a starting point for the main simulation. The box size was chosen to give a water density $\rho = 3$ beads per unit volume far from the bilayer; the overall density was then kept fixed throughout. Then a set of 64

simulations of 10^6 time steps of length $\delta t = 0.01$ was carried out, with temperatures in the range $T = 0.2$–0.6, using parallel tempering and the zero surface tension method. The simulation time step was chosen as a compromise between efficiency and maintaining the equilibrium Boltzmann distribution [25, 31, 32]. The average area per lipid A_{L}, average bilayer thickness d_{L}, and average lipid tail order S_{tail} of the DPPC lipid bilayer were monitored as a function of temperature (see Figure 1). The expected behaviour is seen in all these three quantities. The area per lipid increases, and the bilayer thickness decreases, with increasing temperature (at constant, zero, surface tension). The tail order parameter S_{tail} is approximately constant, at a different value, in each of the low-temperature phases, but shows a progressive decrease with increasing temperature in the fluid phase. Phase transitions were identified by changes of slope of the measured properties of the lipid bilayer. The sequence of phases and transition temperatures were in good agreement with those found by Kranenburg and Smit [17] for the same head-group repulsion parameter $a_{hh} = 35$:

$$\text{fluid } L_\alpha \xrightarrow{T=0.5} \text{ripple } P_{\beta'} \xrightarrow{T=0.37} \text{gel } L_{\beta'} \xrightarrow{T=0.26} \text{sub-gel } L_c$$

The configurations from these runs were modified by inserting two WALP23 peptides into the lipid bilayer at various separations; subsequent runs employed 207 lipid molecules and 7207 water beads, with the same overall density as before. The umbrella potential described in section 3 was applied, with the center-center separation parameter chosen at intervals $\Delta r_{\mathrm{U}} = 0.1$ up to a maximum of half the box length. For each separation, 64 replicas of the system covering the same temperature range as before, were simulated at zero surface tension and constant density for 2×10^6 time steps of $\Delta t = 0.05$;

a multiple-timestep integration algorithm with four sub-steps $\delta t = 0.0125$ [33] was employed for the bond stretching and bending degrees of freedom.

The lipid bilayer properties are again shown in Figure 1, and phase transitions identified by the changes of slope. There is a small shift to lower temperatures, compared with the pure bilayer, induced by the presence of the two peptides, but the effect of peptide separation is very limited. Only in the gel and subgel phases, when the peptides are very close, is there a significant effect of separation on the tail ordering of lipids. Our estimates of the transition temperatures are

$$\text{fluid } L_\alpha \xrightarrow{T=0.47} \text{ripple } P_{\beta'} \xrightarrow{T=0.34} \text{gel } L_{\beta'} \xrightarrow{T=0.23} \text{sub-gel } L_c$$

Snapshots of the peptides in the four different lipid bilayer phases are shown in Fig. 2.

The tilt angle $\chi_{\rm tilt}$, with respect to the lipid bilayer normal, of one of the WALP23 peptides is shown in Figure 3. We see very little systematic dependence on peptide separation, so the results in the main graph are averaged over the different values of $r_{\rm U}$. At low temperatures, gel and sub-gel phases, and in the ripple phase, the peptides reside in the lipid bilayer at small but significant angles. The tilt at low temperatures reflects the equilibrium structure of the bilayer. At higher temperatures, in the fluid phase of the lipid bilayer, the decreasing cosine (increasing average tilt) reflects the larger fluctuations about normal alignment. Changes in behaviour occur at the same temperatures as the phase changes of the lipid bilayer.

The thickness $d_{\rm L}(R)$ of the lipid bilayer around the WALP23 peptide is shown as a function of R at different temperatures in Figure 4. These results are obtained by averaging over configurations for well-separated peptides.

The curves are consistent with a hydrophobic *deficit* (peptide shorter than bilayer thickness) which deforms the bilayer in the vicinity of the peptide. Similar effects were investigated for a variety of examples of hydrophobic mismatch in Ref. [26]. Also shown in the figure are the average lipid thickness values $d_{\rm L}$ at the corresponding temperatures, as reported in Fig. 1. These are a few percent lower than the limiting large-R values of $d_{\rm L}(R)$ due to finite-size effects: they include the regions around the two peptides.

The main target of the present paper is the potential of mean force (PMF). As described before, we used WHAM to combine the different histograms from different separation windows at each temperature, giving an overall probability distribution for the peptide separation, and hence the free energy. The resulting PMF is shown as a function of peptide separation and temperature in Figure 5. Slices through the surface at selected temperatures are shown in Figure 6. This is broadly in accord with the phase transitions in the lipid bilayer; in particular the low-temperature phases show a significant medium-range lipid-induced structure. There is a significantly oscillatory structure to the PMF in all phases, due to the packing of lipid molecules in between the peptides. These oscillations are of longer range in the lower temperature phases.

5. Conclusions

The aim of this brief report has been to illustrate that it is possible to extend the measurement of peptide interactions within a lipid bilayer by computer simulation into the lower-temperature gel phases. Very simple models of the WALP23 peptide within a DPPC membrane [26] were adopted, and

a set of dissipative particle dynamics simulations were run, with the cross-sectional area of the periodic box allowed to vary so as to maintain zero surface tension. Simulation efficiency was enhanced by umbrella sampling with respect to peptide separation, combined with parallel tempering (replica exchange) in temperature. The distributions obtained by umbrella sampling were combined using the WHAM algorithm. Phase transitions were shown clearly in the discontinuity of several properties of the bilayer, and were in accord with previous studies, making a small allowance for finite-size effects and the influence of the peptides on the bilayer. The peptides studied were shown to have a hydrophobic mismatch with the bilayer, causing a contraction of bilayer thickness in their vicinity. The interaction between the peptides was shown to be strongly oscillatory, due to packing of lipids in between them at short distances, and these oscillations persisted to larger separations in the lower-temperature gel phases. In principle, the resulting PMF can then be used to obtain a better understanding of membrane-mediated interactions [34], and this could be the subject of a future study.

One potential limitation of these results is imposed by the finite size of the simulation box. The transverse linear dimensions in this work are of the order of 8–9 bead diameters; systems approximately twice or three times as wide have been used to study, respectively, the phase diagram and the PMF in the high-temperature phase [17, 19]. This means that the results, particularly at larger peptide separations, may be suspect. The compensating factor is that a large number of parallel runs could be undertaken for these relatively small systems, allowing a high degree of overlap between the distributions at neighbouring temperatures and separations.

6. Acknowledgments

Computing facilities were provided by the Centre of Scientific Computing of the University of Warwick with support from SRIF. Funding was provided by EPSRC. I. A. acknowledges a summer visit support from the King Abdulaziz City for Science and Technology and thanks the University of Warwick for hosting his visit.

References

[1] R. B. Gennis, Biomembranes, Molecular Structure and Function, Springer, New York, 1989.

[2] H. Lodish, A. Berk, C. A. Kaiser, M. Krieger, M. P. Scott, A. Bretscher, H. Ploegh, P. Matsudaira, Molecular Cell Biology, W. H. Freeman, 6th edition, 2007.

[3] C. L. Armstrong, E. Sandqvist, M. C. Rheinstaedter, Protein-protein interactions in membranes, Prot. Pep. Lett. 18 (2011) 344–353.

[4] J. Israelachvili, H. Wennerstrom, Role of hydration and water structure in biological and colloidal interactions, Nature 379 (1996) 219–225.

[5] E. Strandberg, S. Esteban-Martin, A. S. Ulrich, J. Salgado, Hydrophobic mismatch of mobile transmembrane helices: Merging theory and experiments, Biochim. Biophys. Acta Biomembranes 1818 (2012) 1242–1249.

[6] B. de Kruijff, J. Killian, D. Ganchev, H. Rinia, E. Sparr, Striated domains: self-organizing ordered assemblies of transmembrane alpha-helical peptides and lipids in bilayers, Biol. Chem. 387 (2006) 235–241.

[7] A. R. Leach, Molecular Modelling: Principles and Applications, Prentice Hall, 2nd edition, 2001.

[8] P. van der Ploeg, H. J. C. Berendsen, Molecular dynamics simulation of a bilayer membrane, J. Chem. Phys. 76 (1982) 3271–3276.

[9] J. Gumbart, Y. Wang, A. Aksimentiev, E. Tajkhorshid, K. Schulten, Molecular dynamics simulations of proteins in lipid bilayers, Curr. Opin. Struct. Biol. 15 (2005) 423 – 431.

[10] M. Venturoli, M. M. Sperotto, M. Kranenburg, B. Smit, Mesoscopic models of biological membranes, Physics Reports 437 (2006) 1–54.

[11] E. Lindahl, M. S. P. Sansom, Membrane proteins: molecular dynamics simulations, Curr. Opin. Struct. Biol. 18 (2008) 425 – 431.

[12] M. L. Berkowitz, J. T. Kindt, Molecular detailed simulations of lipid bilayers, Rev. Comput. Chem. 27 (2010) 253–286.

[13] E. Sparr, W. Ash, P. Nazarov, D. Rijkers, M. Hemminga, D. Tieleman, J. Killian, Self-association of transmembrane alpha-helices in model membranes - importance of helix orientation and role of hydrophobic mismatch, J. Biol. Chem. 280 (2005) 39324–39331.

[14] W. Ash, T. Stockner, D. Tieleman, Replica exchange molecular dynamics studies of helix-helix interactions in membrane proteins, Biophys. J.

88 (2005) 152A. 49th Annual Meeting of the Biopysical-Society, Long Beach, CA, FEB 12-16, 2005.

[15] S. Park, T. Kim, W. Im, Transmembrane helix assembly by window exchange umbrella sampling, Phys. Rev. Lett. 108 (2012) 108102.

[16] W. Shinoda, R. DeVane, M. L. Klein, Computer simulation studies of self-assembling macromolecules, Curr. Opin. Struct. Biol. 22 (2012) 175 – 186.

[17] M. Kranenburg, B. Smit, Phase behavior of model lipid bilayers, J. Phys. Chem. B 109 (2005) 6553–6563.

[18] J. M. Rodgers, J. Sorensen, F. J. M. de Meyer, B. Schiott, B. Smit, Understanding the phase behavior of coarse-grained model lipid bilayers through computational calorimetry, J. Phys. Chem. B 116 (2012) 1551–1569.

[19] F. J.-M. de Meyer, M. Venturoli, B. Smit, Molecular simulations of lipid-mediated protein-protein interactions, Biophys. J. 95 (2008) 1851–1865.

[20] B. West, F. L. H. Brown, F. Schmid, Membrane-protein interactions in a generic coarse-grained model for lipid bilayers, Biophys. J. 96 (2009) 101–115.

[21] E. Psachoulia, D. P. Marshall, M. S. P. Sansom, Molecular dynamics simulations of the dimerization of transmembrane alpha-helices, Acc. Chem. Res. 43 (2010) 388–396.

[22] F. J. M. de Meyer, J. M. Rodgers, T. F. Willems, B. Smit, Molecular simulation of the effect of cholesterol on lipid-mediated protein-protein interactions, Biophys. J. 99 (2010) 3629–3638.

[23] J. Neder, B. West, P. Nielaba, F. Schmid, Membrane-mediated protein-protein interaction: A monte carlo study, Curr. Nanosci. 7 (2011) 656–666.

[24] R. D. Groot, P. B. Warren, Dissipative particle dynamics: Bridging the gap between atomistic and mesoscopic simulation, J. Chem. Phys. 107 (1997) 4423–4435.

[25] P. Espanol, P. Warren, Statistical mechanics of dissipative particle dynamics, Europhys. Lett. 30 (1995) 191–196.

[26] M. Venturoli, B. Smit, M. M. Sperotto, Simulation studies of protein-induced bilayer deformations, and lipid-induced protein tilting, on a mesoscopic model for lipid bilayers with embedded proteins, Biophys. J. 88 (2005) 1778–1798.

[27] S. Morein, J. Killian, M. Sperotto, Characterization of the thermotropic behavior and lateral organization of lipid-peptide mixtures by a combined experimental and theoretical approach: Effects of hydrophobic mismatch and role of flanking residues, Biophys. J. 82 (2002) 1405–1417.

[28] D. J. Earl, M. W. Deem, Parallel tempering: theory, applications, and new perspectives, Phys. Chem. Chem. Phys. 7 (2005) 3910–3916.

[29] Y. Sugita, Y. Okamoto, Replica-exchange molecular dynamics methods for protein folding, Chem. Phys. Lett. 314 (1999) 141–151.

[30] B. Roux, The calculation of the potential of mean force using computer-simulations, Comput. Phys. Commun. 91 (1995) 275–282.

[31] A. F. Jakobsen, O. G. Mouritsen, G. Besold, Artifacts in dynamical simulations of coarse-grained model lipid bilayers, J. Chem. Phys. 122 (2005) 204901.

[32] M. P. Allen, Configurational temperature in membrane simulations using dissipative particle dynamics, J. Phys. Chem. B 110 (2006) 3823–3830.

[33] A. F. Jakobsen, G. Besold, O. G. Mouritsen, Multiple time step update schemes for dissipative particle dynamics, J. Chem. Phys. 124 (2006) 094104.

[34] M. Yiannourakou, L. Marsella, F. de Meyer, B. Smit, Towards an understanding of membrane-mediated protein-protein interactions, Faraday Disc. Chem. Soc. 144 (2010) 359–367.

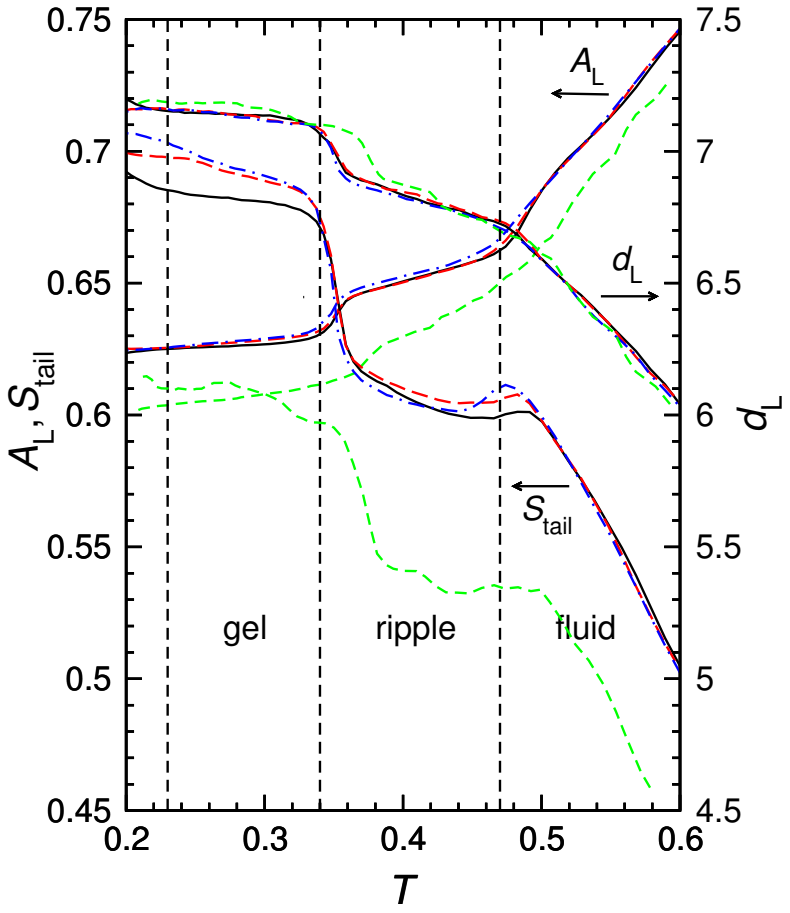

Figure 1: Area per lipid A_{L}, bilayer thickness d_{L} and lipid tail order S_{tail} of the DPPC lipid bilayer with two WALP23 peptides at selected separations: black (solid line): $r_{\mathrm{U}} = 1.0$; red (long-dashed line): $r_{\mathrm{U}} = 3.0$; blue (dot-dashed line): $r_{\mathrm{U}} = 5.0$. Also shown in green (short-dashed line) are the results for the pure lipid bilayer. Vertical dashed lines mark the approximate locations of the phase transitions in the lipid membrane in the presence of the two peptides.

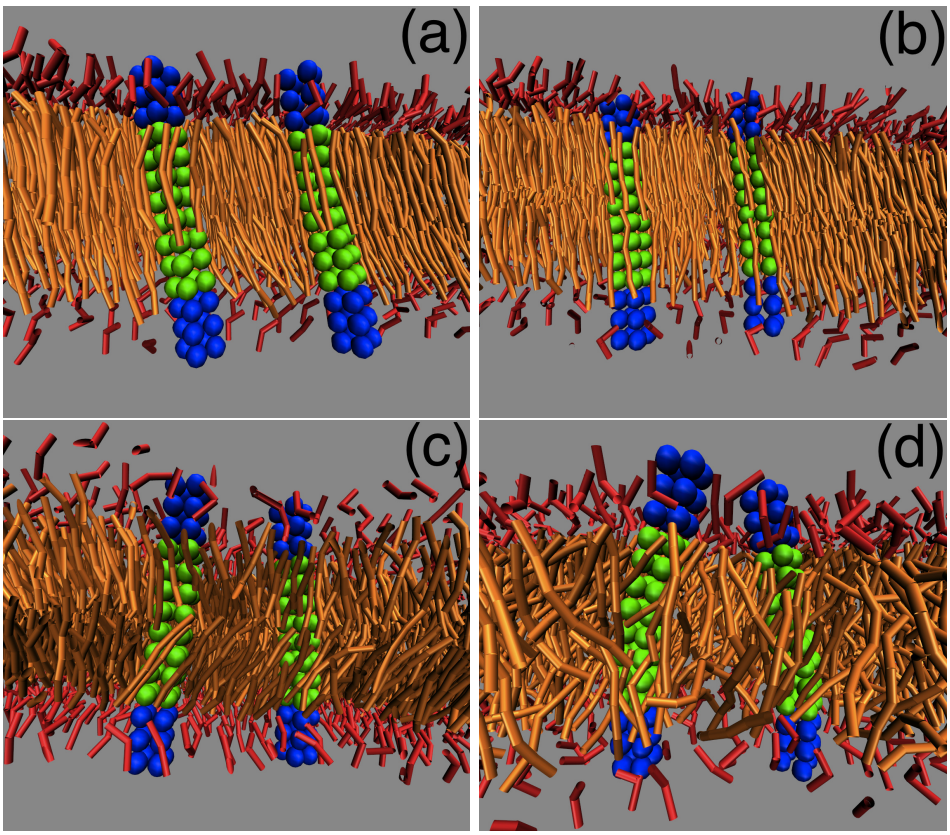

Figure 2: Snapshots of the WALP23 peptides in the DPPC lipid bilayer. (a) sub-gel phase, $T = 0.22$; (b) gel, $T = 0.32$; (c) ripple, $T = 0.43$; (d) fluid, $T = 0.55$. For clarity, water has been omitted, and the lipids are represented by thin cylinders. Only the immediate vicinity of the peptides is shown. Colour coding: lipid hydrophilic head beads h (red), lipid hydrophobic tail beads t (orange), peptide hydrophilic end beads p (blue), and peptide hydrophobic internal beads q (green).

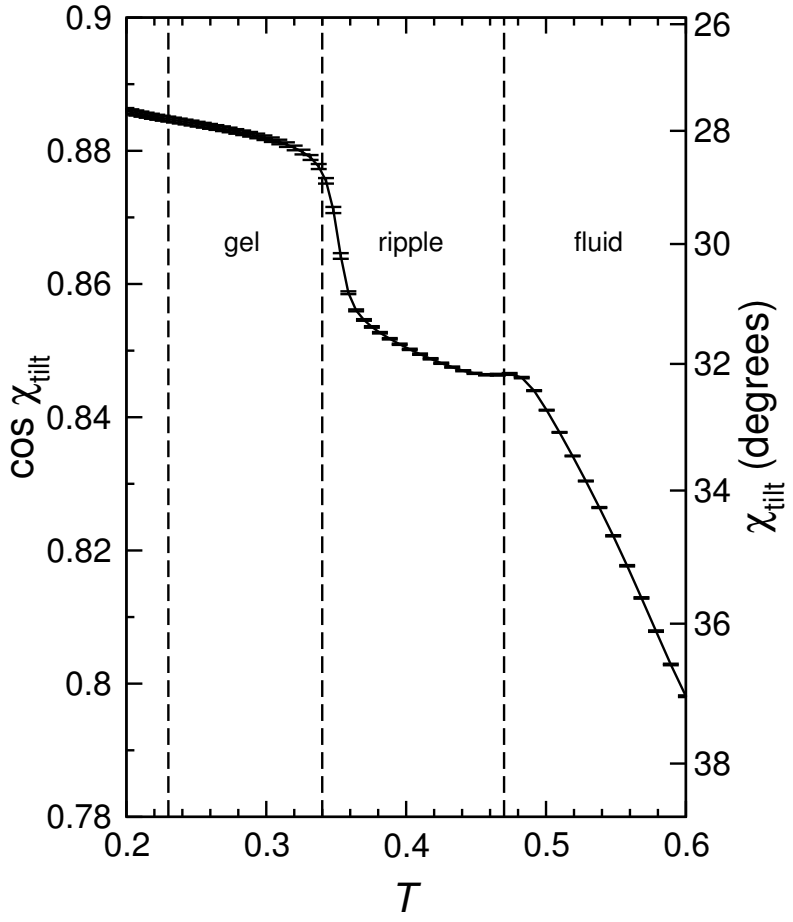

Figure 3: Tilt angle $\chi_{\rm tilt}$ between the lipid bilayer normal and the longitudinal axis of one of the peptides, as a function of temperature T.

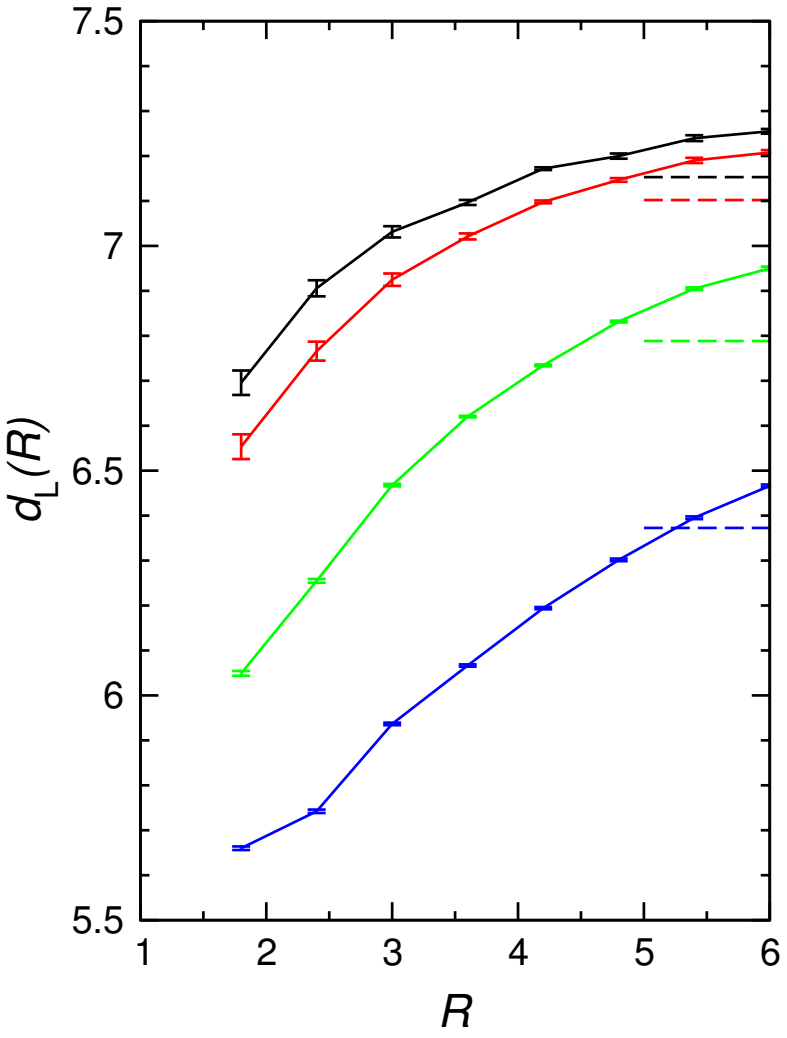

Figure 4: The average hydrophobic thickness of the lipid bilayer $d_{\mathrm{L}}(R)$ around one of the WALP23 peptides as a function of distance from the peptide R. Temperatures, top to bottom: $T = 0.200$ (sub-gel phase, black), 0.320 (gel, red), 0.425 (ripple, green), 0.538 (fluid, blue). Dashed lines indicate the average lipid thickness for the whole system at the corresponding temperatures (see Fig. 1).

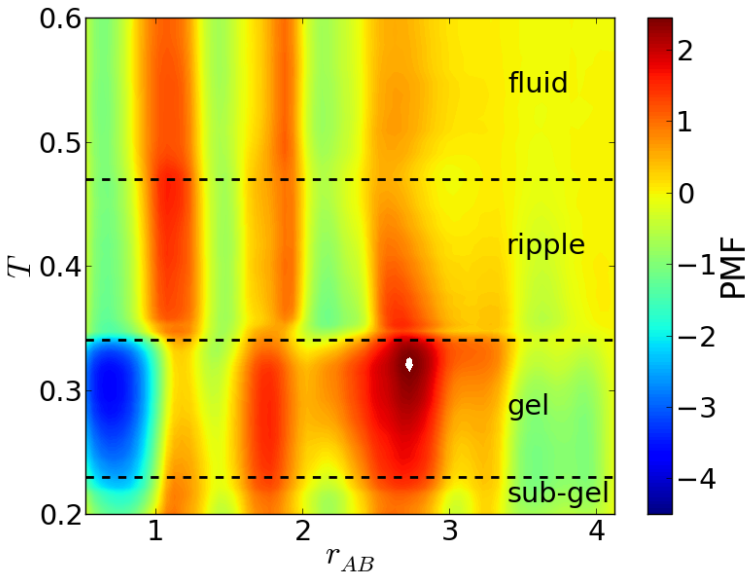

Figure 5: The potential of mean force (PMF) as a function of peptide separation r_{AB} and temperature T. Dashed lines show the phase transition temperatures.

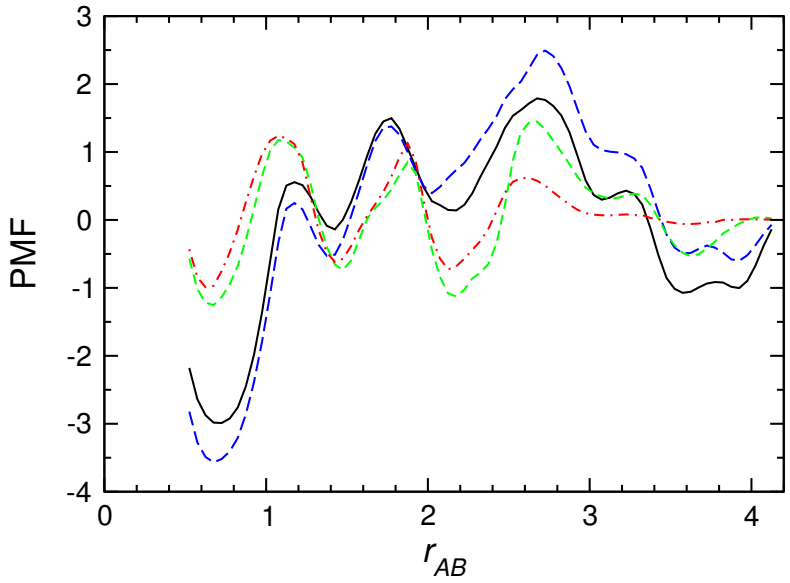

Figure 6: The potential of mean force (PMF) as a function of peptide separation r_{AB} at selected temperatures: $T = 0.25$, gel phase (black, solid line); $T = 0.32$, gel phase (blue, long-dashed line); $T = 0.36$, ripple phase (green, short-dashed line); $T = 0.50$, liquid phase (red, dot-dashed line).